doi:10.4028/www.scientific.net/MSF.790-791.435

A possible mechanism for the formation of exploded graphite in nodular cast irons

Roxana Ghergu[1,a], Lena Magnusson Åberg[2,b], Jacques Lacaze[1,c]

[1]CIRIMAT, ENSIACET, Université de Toulouse, B.P. 44362, 31030 Toulouse cedex 4,France

[2]ELKEM AS, Foundry Technology Products R&D, P.O. Box 8040 Vaagsbygd, N-4675 Kristiansand S, Norway

[a]gherguroxana@yahoo.com, [b]lena.magnusson.aberg@elkem.no, [c]jacques.lacaze@ensiacet.fr

Keywords: spheroidal graphite, primary growth, graphite degeneracy, exploded graphite

Abstract. In hypereutectic nodular cast irons, primary precipitation of graphite may lead to graphite flotation in thick section castings. Graphite degeneracy such as so-called exploded graphite is then often associated with this flotation phenomenon and it appears as precipitates where the nodular form is replaced by star-like or flower-like shape. It has been reported that exploded graphite develops after the primary spheroidal nodules have reached some tens of microns in diameter. In this contribution, a model for this transition is presented.

Introduction

The most reliable observation of the formation of exploded graphite in hypereutectic nodular cast irons describes it in two steps: the growth of a normal spheroid which then evolves with the formation and development of protuberances as illustrated in Fig. 1 [1, 2]. Owing to the shape of the protuberances, Sun and Loper [2] differentiated flower, star and snow flake shaped exploded graphite. The change from a spheroid to a branched structure has led some authors to consider that this transition is due to a Mullins-Sekerka shape instability but this claim may be ruled out because very large highly spherical nodules have been observed with sizes far above the Mullins-Sekerka critical size which has been estimated to 300-500 Å for an undercooling of 150°C [3].

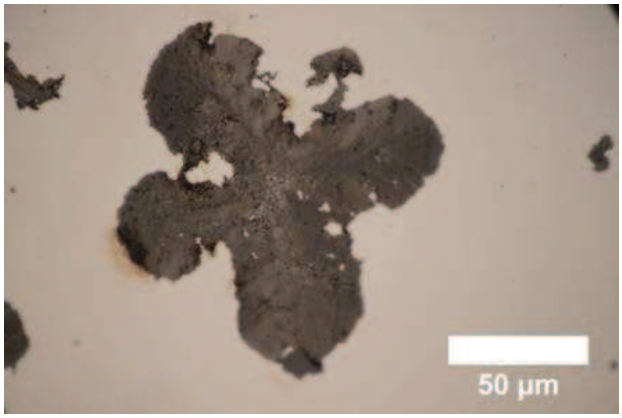

Fig. 1. Example of exploded graphite in a hypereutectic cast iron.

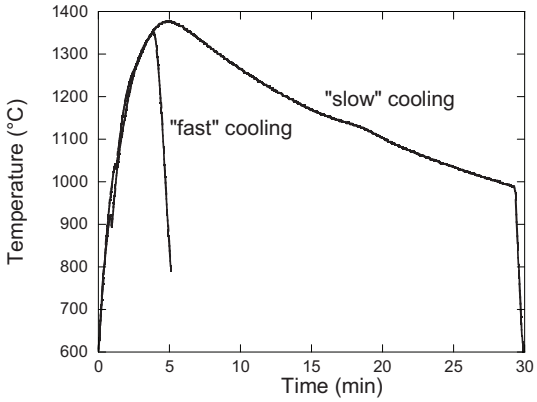

Fig. 2. Examples of temperature-time records during melting and solidification.

In this work, we first shortly present experimental laboratory results that allowed studying growth of exploded graphite. Then, we present a new mechanism for the formation of exploded graphite which is based on recent observations showing that spheroidal growth of graphite in cast irons does not proceed by a spiral growth process [4]. Instead, this growth should proceed by lateral extension of new graphite layers nucleated at the outer surface of the nodules, in agreement with one of the models proposed by Double and Hellawell [5]. From this, a simple schematic is suggested that allows predicting the transition from spheroidal to exploded growth.

Experimental details

A cast iron with 3.75 wt.% C and 2.7 wt.% Si was remelted in graphite crucibles (ALPHA AR6247 designed for chemical analysis of oxygen and nitrogen) by heating up to 1350°C and then cooled at 20°C/min or 350-400°C/min in a facility that has been described previously [6]. These cooling rates will be referred to as slow and fast cooling respectively. The samples were 1 cm in height and 8 mm in diameter and commercial inoculant amounting to 0.2% of their weight was located at the bottom of the crucible. Heating was performed under vacuum for the first 1.5 minute and then under a low flow of argon. Fig. 2 shows examples of the temperature-time records made with a thermocouple located below the crucible.

Samples were sectioned afterwards along a vertical axial section and prepared for metallographic observations.

Results

Melting in a graphite crucible increased the carbon content of the alloy which then became hypereutectic. Fig. 3 shows example of the upper part of the section of a fast (a) and a slow (b) cooled samples where relatively large and small graphite precipitates can be observed. The large precipitates are associated with primary graphite growth while the small ones formed during the eutectic reaction. Large precipitates were not numerous for the fast cooled samples and were most often evenly distributed in the volume, though limited flotation was sometimes observed as in Fig. 3-a. In slow cooled samples, a large flotation zone with much more numerous precipitates was observed (Fig. 3-b). It is also seen in Fig. 3 that many of these large precipitates show a degenerate form of spheroidal graphite.

Upon cooling down from the maximum temperature to the temperature where bulk eutectic reaction took place, the large precipitates nucleated at the bottom of the sample, then grew at the same time as they floated towards the top of the sample. The half-size of the five largest precipitates in the various samples that have been prepared was measured and the ranges of obtained values are shown in Fig. 4.

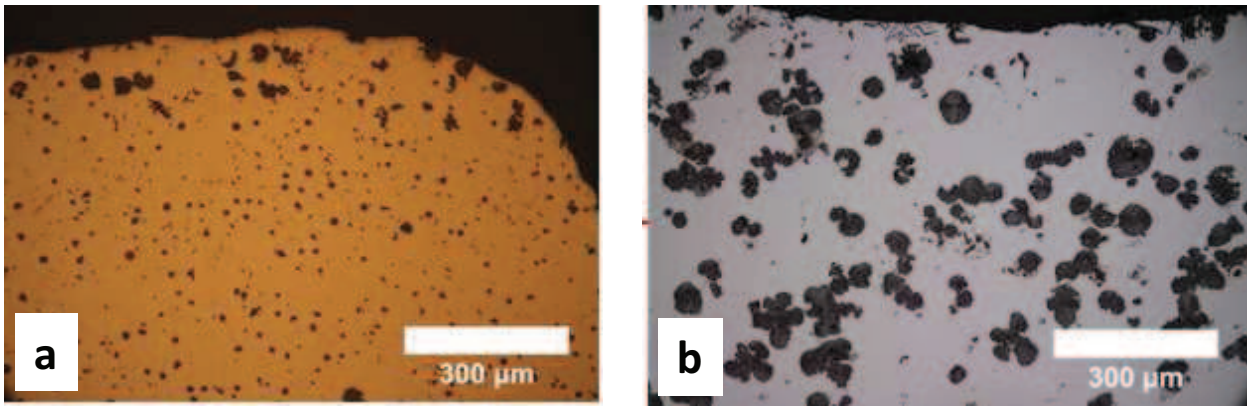

Fig. 3. Upper part of the vertical section of fast (a) and slow (b) cooled samples.

Discussion

Overall growth kinetics of graphite spheroids. In a previous work on modelling solidification of hypo- and hyper-eutectic nodular cast irons [7, 8] primary deposition of graphite spheroids was described considering both diffusion of carbon in the liquid and chemically controlled carbon transfer at the liquid graphite interface. The flux density of carbon ϕ related to this latter chemical reaction was written:

$$\phi = -K \cdot \rho^{1} \cdot \left(w_C^{i} - w_C^{1/g} \right)^2 \qquad (1)$$

where K is a constant characteristic of the chemical reaction, ρ^l is the liquid density, w_C^i is the carbon content (mass fraction) in the liquid at the interface and $w_C^{l/g}$ is the carbon content (mass fraction) in the liquid at thermodynamic equilibrium with graphite. For K varying between 10^{-4} and 1 $m.s^{-1}$ the growth of graphite spheroids changed from a full control by the interfacial reaction to a near purely diffusive regime. The growth rate of a graphite spheroid of radius R^g is then given as:

$$\frac{dR^g}{dt} = K \cdot \frac{\rho^l}{\rho^g} \cdot \frac{\left(w_C^i - w_C^{l/g}\right)^2}{1 - w_C^i} \tag{2}$$

where ρ^g is the density of graphite and w_C^i is written as:

$$w_C^i = w_C^{l/g} + \sqrt{\left(\frac{D_C^l}{2 \cdot K \cdot R^g}\right)^2 + \frac{D_C^l}{K \cdot R^g} \cdot \left(w_C^\infty - w_C^{l/g}\right)} - \frac{D_C^l}{2 \cdot K \cdot R^g} \tag{3}$$

where w_C^∞ is the far-field carbon content in the liquid and D_C^l is the diffusion coefficient of carbon in the liquid.

In this previous work [7,8], K was finally set to 10^{-2} $m.s^{-1}$ on the basis of post-mortem measurements of nodule counts associated to primary graphite precipitation, whilst the simulation included a continuous nucleation law and an overall mass balance for evaluation of the carbon content in the remaining liquid. Instead, calculation were here performed to evaluate the largest size of the spheroids that could be observed and that were assumed to have nucleated at the very first stage of cooling and have grown in a liquid with a constant carbon content given by the graphite liquidus at the upper holding temperature ($T_L^g(°C) = -534.5 + 389.0 \cdot w_C$, where w_C is here in wt.% [8]). Calculations shown in Fig. 4 were performed with all data as before [7, 8] but K set here at $5 \cdot 10^{-2}$ $m.s^{-1}$. This latter value was selected to give a good fit with particle size obtained at 350 K/min while growth at low cooling rate was affected by the clustering due to settling, leading to experimental values lower than expected.

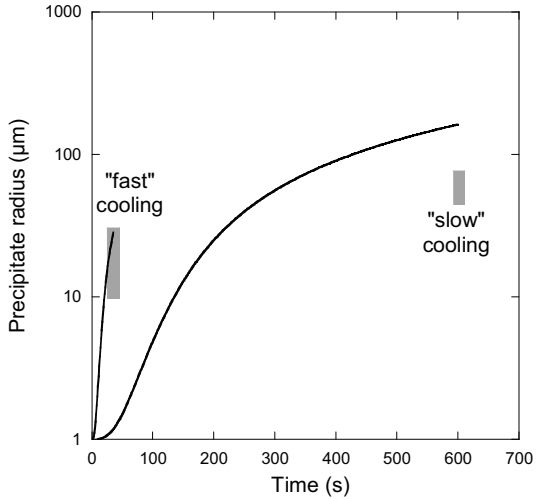

Fig. 4. Greyed areas illustrate the range of half-size values of the precipitates in fast and slow cooled samples plotted versus the time to cool the melt from 1350°C to 1150°C. Solid lines show the evolution during cooling from 1350 to 1150°C of the radius of a primary graphite spheroid calculated for two cooling rates, 20 K/min and 350 K/min.

Mechanism of spheroidization. Lamellar and spheroidal graphite, and other forms of graphite found in cast irons do consist in structural base units (SBU) that are stacks of graphene layers elongated in the ***a*** direction, with a thickness typically of 50-500 nm and a length of a couple of micrometres. These SBUs do have quite a high crystalline quality. The resulting internal structure of graphite, in lamellae of flake graphite as well as in sectors of spheroids, appears as illustrated in Fig. 5, with SBUs being tilted between each other around the ***c*** axis [9].

It should be noted that the internal structure of sectors in spheroidal graphite as schematically illustrated in Fig. 5 rules out any mechanisms invoking growth around spiral dislocations as stressed recently on the basis of TEM examination [6]. Instead, following the model developed by Double and Hellawell [5], it is suggested that SBUs in spheroidal graphite result from repeated nucleation at

the outer surface of the spheroids, which then expand in the prismatic directions alongside the spheroid surface. It should be considered that the graphite growth rate then remains higher along the prismatic direction than along the basal direction in this schematic in agreement with the relative binding energies on these two types of planes. Assuming nuclei of new SBUs are disk shaped with radius r and height h, the free enthalpy change ΔG writes:

$$\Delta G = \pi \cdot r^2 \cdot h \cdot \frac{\Delta G_m}{V_m} + 2 \cdot \pi \cdot r \cdot h \cdot \sigma_p \qquad (4)$$

where ΔG_m and V_m are the molar Gibbs energy and volume of graphite, and σ_p is the surface energy of the prismatic planes assumed independent of orientation. The critical radius (r*) is obtained by differentiating the above equation:

$$r^* = \frac{\sigma_p}{-\Delta G_m / V_m} \qquad (5)$$

while the height can be of any value and is most often taken as one atomic distance. It is suggested here to estimate it with its value for homogeneous nucleation of graphite [10]:

$$h^* = \frac{4 \cdot \sigma_b}{-\Delta G_m / V_m} \qquad (6)$$

where σ_b is the surface energy of the basal planes. Using $-\Delta G_m = 3.26 \cdot \Delta T$ (cal/mol) $= 13.64 \cdot \Delta T$ (J/mol) as given by Hillert [10], and with $V_m = 5.31$ cm^3/mol and $\sigma_b = \sigma_p \approx 1.5 \cdot 10^{-4}$ J/cm^2 [11], one gets: $h^* = 4 \cdot r^* = 2.3 \cdot (\Delta T)^{-1}$ μm.

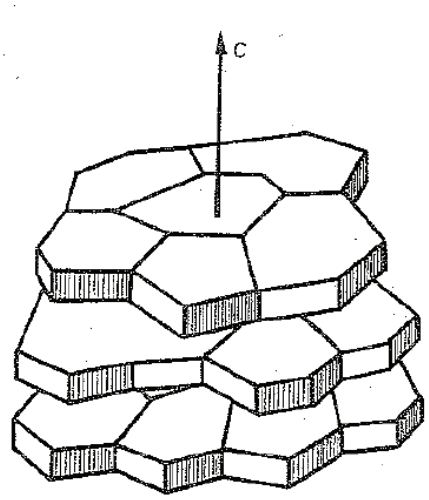

Fig. 5. Schematic of the graphite structure in a sector of a spheroid (after Mitsche et al. [9]).

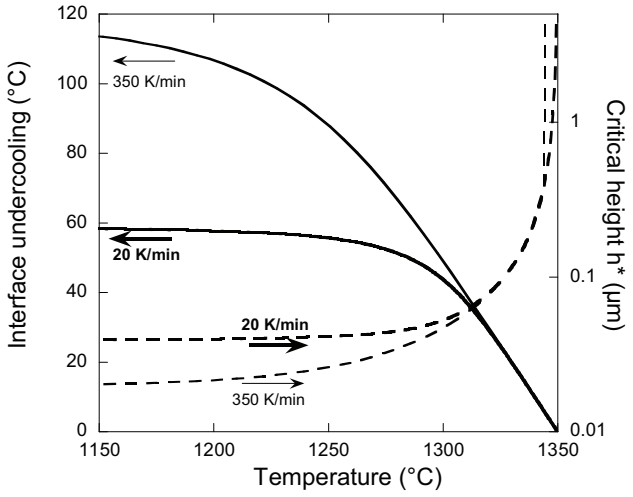

Fig. 6. Evolution with temperature of the graphite/liquid interface undercooling (solid lines) and critical height (interrupted lines) upon cooling at 20 and 350 K/min.

Using the $K = 5 \cdot 10^{-2}$ m/s, calculation of the evolution of r* and h* during growth of the spheroids (eq. 2) was performed for the present cooling conditions. The results are shown for the two cooling rates in Fig. 6. It is seen that the undercooling of the graphite/liquid interface with respect to the graphite liquidus increases to 58°C and 115°C for cooling rate of 20 and 350°C/min, respectively. After a sharp decrease, the critical height stabilizes at 0.04 and 0.02 μm, or 40 and 20 nm, respectively. These values compare well with the reported thickness of SBUs while the values of r* are 100 times lower than their lateral extension, thus leaving place for a significant growth stage after nucleation.

Mechanism leading to the development of exploded graphite. The mechanisms by which the spheroidizing elements Mg and Ce affect graphite growth are certainly similar in view of their

spheroidizing effect and their propensity to also generate exploded graphite, though the effectiveness of Mg seems lower than that of Ce [2]. There is little doubt that Mg and Ce adsorb at the outer surface of the graphite and this could help the roughening of the graphite/liquid interface that has been claimed for explaining spheroidal growth [12]. It is suggested here that this adsorption may instead trigger nucleation of new SBUs that should then expand laterally to cover the outer surface of spheroid' sectors.

Fig. 7 shows a diametric section of a nodule that has grown spherically for a while. To maintain the "spheroidal" shape, the spreading rate V_a along the ***a*** direction of new SBUs nucleated at the outer surface of each sector should be fast enough so that each SBU has extended over a length of the order of l (see Fig. 7) within the time step δt between each nucleation event. The critical value of this time step is given as $\delta t = h^*/(dR^g/dt)$, where dR^g/dt is the instantaneous growth rate of the spheroid, and one has the following relation: $V_a \cdot \delta t \geq l = 2 \cdot \pi \cdot R^g/n$ where n is the number of sectors seen on a metallographic section of a nodule.

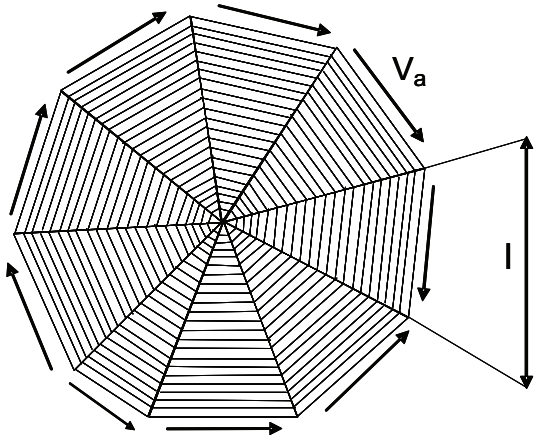

Fig. 7. Diametric section of a graphite nodule showing adjacent sectors.

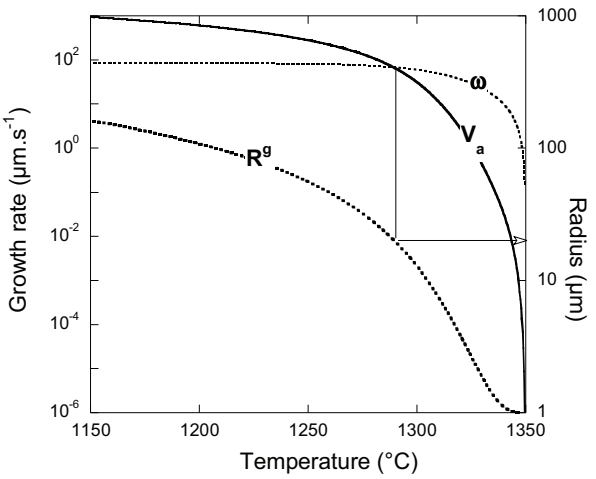

Fig. 8. Calculation of the growth rates ω and V_a as function of melt temperature, for a cooling rate of 20°C/min. The intersection of the V_a and ω curves gives the nodule radius over which protuberances may appear.

The calculation of the critical value of V_a was performed for cooling rates of 20 and 350°C/min, estimating ΔT in the expression of h* as the actual interface undercooling (i.e. using the value of the carbon content at the interface w_C^i). The evolution of V_a has been reported as function of temperature in Fig. 8 for the slow cooling rate. It is there compared with the growth rate w for lamellar graphite from Lesoult [13] which may be expressed as $\omega = 6 \cdot 10^{-7} \cdot \Delta T^{1.22}$ ($m.s^{-1}$) and agrees with data from Fredriksson [14]. It is seen that at high temperature (and low interface undercooling) the critical value V_a is below the w value, meaning the layers have enough time to spread along the spheroid interface, while the opposite is true at lower temperature when the nodules have grown to some extent. In these latter conditions, new layers will form along the liquid/graphite interface before the previous layers have filled the space. The cross-over of the curves is thus a rough estimate of when conditions are fulfilled for protuberances to develop. The values of the graphite radius at the cross-over of the curves are 20 and 7 µm for cooling rate of 20 and 350°C/min, respectively, they do agree with reported observations on exploded graphite.

Conclusion

This work suggests that removing S and O by adding Mg or Ce to cast iron melts leads to easy nucleation of new graphite layers onto the basal planes. An attempt to put numbers on the spheroidal growth resulting from lateral extension of new graphite layers nucleated at the outer surface of the nodules leads to conclude that exploded graphite occurs easily once the spheroids have reached a critical radius that changes from 7 to 20 µm when the cooling rate is increased from 20 to 350°C/min.

References

[1] N.N. Aleksandrov, B.S. Mil'man, N.G. Osada, L.V. Il'icheva, V.V. Andreev, Crystallization and structure of vermicular graphite in cast iron, Russian casting production, 9 (1975) 365-366

[2] G.X. Sun, C.R. Loper, Graphite flotation in cast iron, AFS Trans. 91 (1983) 841-854

[3] W.C. Johnson, H.B. Smartt, The role of interphase boundary adsorption in the formation of spheroidal graphite in cast iron, Metall. Trans 8A (1977) 553-565

[4] K. Theuwissen, M.-C. Lafont, L. Laffont, B. Viguier, J. Lacaze, Microstructural characterization of graphite spheroids in ductile iron, Trans. Indian Inst. Met. 65 (2012) 627-631

[5] D.D. Double, A. Hellawell, The nucleation and growth of graphite. The modification of cast iron, Acta Metall. Mater. 43 (1995) 2435-2442

[6] K. Theuwissen, J. Lacaze, L. Laffont, J. Zollinger, D. Daloz, Effect of Ce and Sb on Primary Graphite Growth in Cast Irons, Trans. Indian Inst. Met. 65 (2012) 707-712

[7] G. Lesoult M. Castro, J. Lacaze, Solidification of spheroidal graphite cast iron. Part I : physical modelling, Acta materialia 46 (1998) 983-995

[8] J. Lacaze, G. Lesoult, M. Castro, Solidification of spheroidal graphite cast iron. Part II: numerical simulation, Acta materialia 46 (1998) 997-1010

[9] R. Mitsche, G. Haensel, K. Maurer, H. Schäffer, Recherches, par examen au microscope électronique notamment, sur les formes dégénérées du graphite dans les fontes G.S., Fonderie 270 (1968) 367-382

[10] M. Hillert, Some theoretical considerations in nucleation and growth during solidification of graphitic and white cast irons, in: H.D. Merchant (Ed.), Recent research on cast iron, Gordon and Breach, New-York, 1968, pp. 101-127

[11] R.H. McSwain, C.E. Bates, W.D. Scott, Iron-graphite surface phenomena and their effects on iron solidification, AFS Trans. 82 (1974) 85-94

[12] S. Amini, R. Abbaschian, Nucleation and growth kinetics of grapheme layers from a molten phase, Carbon 51 (2013) 110-123

[13] G.R. Lesoult, Recherche sur la théorie de la solidification eutectique dirigée, Thèse de doctorat d'Etat, Institut National Polytechnique de Lorraine, France, 1976

[14] H. Fredriksson, S. Wetterfall, A study of transition from undercooled to flake graphite in cast iron, in: B. Lux, I. Minfoff, F. Mollard (Eds.), The Metallurgy of Cast Iron, Georgi Pub. Comp., Saint-Saphorin, 1975, pp. 277-293

Solidification and Gravity VI
10.4028/www.scientific.net/MSF.790-791

A Possible Mechanism for the Formation of Exploded Graphite in Nodular Cast Irons
10.4028/www.scientific.net/MSF.790-791.435

DOI References
[4] K. Theuwissen, M. -C. Lafont, L. Laffont, B. Viguier, J. Lacaze, Microstructural characterization of graphite spheroids in ductile iron, Trans. Indian Inst. Met. 65 (2012) 627-631.
http://dx.doi.org/10.1007/s12666-012-0162-5
[5] D.D. Double, A. Hellawell, The nucleation and growth of graphite. The modification of cast iron, Acta Metall. Mater. 43 (1995) 2435-2442.
http://dx.doi.org/10.1016/0956-7151(94)00416-1
[6] K. Theuwissen, J. Lacaze, L. Laffont, J. Zollinger, D. Daloz, Effect of Ce and Sb on Primary Graphite Growth in Cast Irons, Trans. Indian Inst. Met. 65 (2012) 707-712.
http://dx.doi.org/10.1007/s12666-012-0203-0
[7] G. Lesoult M. Castro, J. Lacaze, Solidification of spheroidal graphite cast iron. Part I : physical modelling, Acta materialia 46 (1998) 983-995.
http://dx.doi.org/10.1016/S1359-6454(97)00281-4
[8] J. Lacaze, G. Lesoult, M. Castro, Solidification of spheroidal graphite cast iron. Part II: numerical simulation, Acta materialia 46 (1998) 997-1010.
http://dx.doi.org/10.1016/S1359-6454(97)00282-6
[12] S. Amini, R. Abbaschian, Nucleation and growth kinetics of grapheme layers from a molten phase, Carbon 51 (2013) 110-123.
http://dx.doi.org/10.1016/j.carbon.2012.08.019